RAA 2020 Vol. **20** No. **12**, 211(10pp) doi: 10.1088/1674-4527/20/12/211

http://www.raa-journal.org *http://iopscience.iop.org/raa*

Research in Astronomy and Astrophysics

The wide-field photometric system of the Nanshan One-meter Telescope

Chun-Hai Bai[1,2], Guo-Jie Feng[1], Xuan Zhang[1], Hu-Biao Niu[1], Abdusamatjan Eskandar[1], Guang-Xin Pu[1], Shu-Guo Ma[1], Jin-Zhong Liu[1], Xiao-Jun Jiang[2], Lu Ma[1], Ali Esamdin[1] and Na Wang[1]

[1] Xinjiang Astronomical Observatories, Chinese Academy of Sciences, Urumqi 830011, China; *baichunhai@xao.ac.cn, fengguojie@xao.ac.cn*

[2] Key Laboratory of Optical Astronomy, National Astronomical Observatories, Chinese Academy of Sciences, Beijing 100101, China

Received 2020 March 30; accepted 2020 June 13

Abstract The Nanshan One-meter Wide-field Telescope is a prime focus system that is located at Nanshan Station of Xinjiang Astronomical Observatories. The field of view was designed to $1.5^\circ \times 1.5^\circ$, and the Johnson-Cousins $UBVRI$ system was chosen as the main filter set. The telescope has been providing observation services for astronomers since September 2013. Variable source searching and time-domain surveys are the main scientific goals. The system's test results are reported including linearity, dark current, bias, readout noise and gain of the CCD camera. The accurate instrumental calibration coefficients in $UBVRI$ bands were driven with Landolt standard stars during photometric nights. Finally, the limiting magnitudes are given with signal-to-noise ratios and various exposure times for observers.

Key words: telescope — filter — CCD photometry

1 INTRODUCTION

The Nanshan One-meter Wide-field Telescope (NOWT) is situated at Nanshan Station (87°10′30″ East, 43°28′25″ North; at an altitude of about 2088m) of Xinjiang Astronomical Observatories (XAO) (Hu et al. 2017, Liu et al. 2014), Chinese Academy of Sciences (CAS). The distribution peak of seeing values around 1.67″, and 80% of the value obtained at nights are below 2.2″. At zenith, the sky brightness is around 21.7 mag arcsec^{-2} in the V-band. The observable night of Nanshan Station is more than 300 days per year, and the clear night is greater than 210, according to the observation records of a 40-cm optical telescope (2005 $\sim$ 2008). Compared to other domestic one meter class telescopes, NOWT has a larger field of view and a higher coverage efficiency in sky survey. At present, the telescope has a mature observation and technical maintenance team. According to the needs of different data reduction, the corresponding pipeline has been completed. The main scientific projects conducted using NOWT after the installation have been multi-color photometry of binaries (Zhang et al. 2018), pulsating stars (Fu et al. 2017), exoplanets (Wang et al. 2018), variable stars (Yang et al. 2018; Bai et al. 2019), gravitational wave (Liu & Zhang 2016), galaxies (Zhang et al. 2015), and surveys (Ma et al. 2018; Zheng et al. 2019).

In March 2012, the telescope was installed by German APM telescope company and XAO optical technicians. It would be useful and significant if observers could be aware of the performance and characteristics of NOWT, including the dark, bias level and linearity of the camera. Besides, the CCD photometric system was analyzed carefully and the results are reported, including the instrument response, throughput and detection limit.

In Section 2, the NOWT observation system is introduced. In Section 3, the specifications of camera are reported. The transformation coefficients and calibration of photometrical system are given in Section 4. In Section 5, we gave the detection limit and throughput. A summary is given in Section 6.

2 PRIME-FOCUS OPTICS AND CAMERA

The NOWT is a horizontal mounting telescope (Figs. 1 and 2). The parabolic primary mirror's effective diameter is 1000 mm, 80% of the collected energy is concentrating into a circle with diameter of less than 1.15″ on a field diameter of 2.4°. The prime focus designed focal ratio is 2.2, but the actually focal length of NOWT is 2159 $\pm$ 20 mm. The mirrors and mount characteristics of NOWT are listed in Table 1. The CCD camera was designed and integrated by the CCD laboratory of the

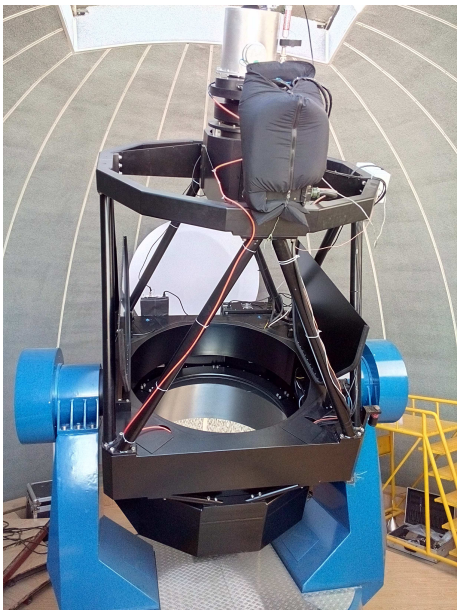

Fig. 1 Front view of NOWT.

Fig. 2 Back view of NOWT.

National Astronomical Observatories of China (NAOC), CAS. The CCD chip model is E2V CCD203–82, and is blue sensitive, with four amplifiers and a 16 bit A/D converter. The spectral response of the chip is shown in Figure 3. The CCD is a scientific-grade chip, but do not have anti-blooming gate. It was made by E2V technologies company, and mounted to NOWT in October of 2012. The specifications of CCD camera are listed in Table 2. It was cooling by liquid nitrogen, the temperature can reach –110°C in summer and –135°C in winter. With a 4096 × 4136 imaging pixels (12 × 12 μm pixel^{-1}), the efficiency field of view (FOV) of the CCD is 78′ × 78′, and the pixel scale is 1.125″. A Johnson-Cousins standard $UBVIR$ filters system that was made by Custom Scientific company started to serve since January of 2013. Whenever needed, time synchronization is realized through networks which was built based on a local GPS time server.

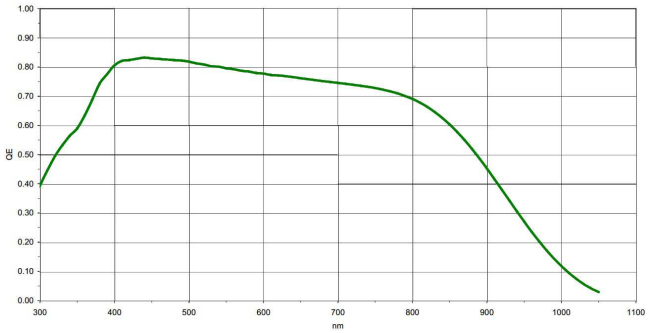

Fig. 3 The spectral response of chip is shown as the solid green line.

3 CAMERA CHARACTERISTICS

3.1 Bias

We can get the original bias image with over scan in Figure 4. To make the over scan region more obvious, we used the 2k × 2k image. When the ambient temperature changes relatively large, the bias value also changes slightly. So we set 32 column under scan pixels for each amplifier, one can use the over scan to correct image data. Bias level of different reading speed and gain setting were tested on the night of 2017 June, we take 10 bias images for each model. The bias images which corrected by overscan was shown in Figure 5. We can see that the proceeded image was acceptable.

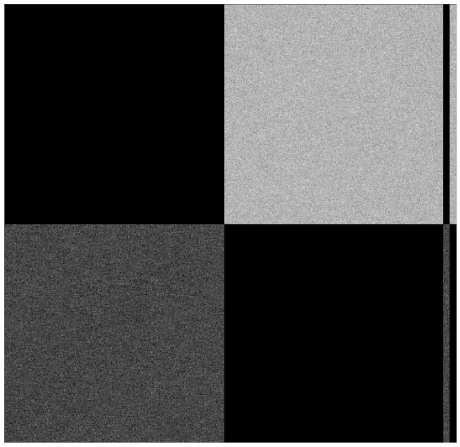

Fig. 4 Bias image with over scan of four amplifiers.

The bias stability of the chip was tested in the evening of 2017 September, when the temperature of CCD chip is lower than –100°C. As shown in Figure 6, the bias changed slightly when the temperature of CCD chip dropped from

Table 1 Characteristics of the NOWT Mirrors and Mount

Features	Characteristics
effective diameter	1000 mm
prime focal length	2200 mm
FOV at prime focus	$1.5^\circ \times 1.5^\circ$
Efficiency of prime focus	87.46%
primary mirror material	Schott Zerodur
maximum slew speed	$>7^\circ\ s^{-1}$ (both axes)
maximum accelerations Azimuth	$>1.8^\circ\ s^{-2}$
maximum accelerations Altitude	$>1.3^\circ\ s^{-2}$
pointing accuracy RMS-Error of RA	$2.4''$
pointing accuracy RMS-Error of DEC	$3''$
tracking accuracy RA	$1.8''$RMS in 60 min
tracking accuracy DEC	$1.8''$RMS in 60 min
zenith blind hole	$<2^\circ$
Rotation angle on Azimuth	$\pm\ 289^\circ$
Rotation angle on Elevation	$7.5^\circ \sim 90.7^\circ$
rotater angle	$\pm\ 180^\circ$
maximum rotation speed	$2^\circ\ s^{-1}$
focus accuracy	1 μm

Table 2 Specifications of the Chip According to the Manual

Features	Specifications
Pixel number	4096×4136
Pixel size	12 μm × 12 μm
Pixel scale	$1.125''$
Imaging area	49.2 mm × 49.6 mm
Effective FOV	$78' \times 78'$
Fill factor	100%
A/D conversion	16 bit
Number of output amplifiers	4
Number of serial registers	2
Number of serial underscan pixels	50
Shortest exposure time	100 ms
Full well (min ∼ typical)	$130\,000 \sim 175\,000\ e^-\ pixel^{-1}$
Scan rates (Fast, Medium, Slow)	146 kHz, 91 kHz, 51 kHz
Full frame readout time	27s@146 kHz, 44s@91 kHz, 78s@51 kHz
Operating temperature	–100°C ∼ –130°C
Readout noise	$3 \sim 4.5e^-$
Dark current ($e^-\ pixel^{-1}\ h^{-1}$)	3 @ –100°C, 0.01 @ –120°C
Linearity	> 99.9995 %
Spectral range	300 ∼ 1060 nm
Peak quantum efficiency	90 %

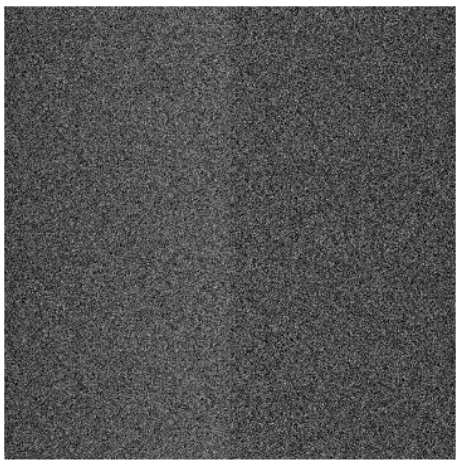

Fig. 5 Four amplifiers bias corrected by overscan, the ADU is uniform.

–117°C to –121°C. Because the CCD has four gates, we have tested the stability of the four amplifiers. UL, UR, DL and DR represents the up left amplifier, the up right amplifier, the lower left amplifier and the lower right amplifier respectively. TDET represents the temperature of detector. One can see that the bias values of the four amplifiers are very stable on their respective Analog-to-Digital (ADU). The ADU of the four amplifiers is different because the gain of the four gates is slightly different, which will be described in detail in the gain section that follows. The scan rates and gain selection were set to Medium and 1x, because many observers use this selection.

3.2 Readout Noise and Gain

The gain (G) is useful for observer to evaluate the camera's performance. It is also the factor that describes how many the digital outputs are converted into one unit electrons. The readout noise and gain values were

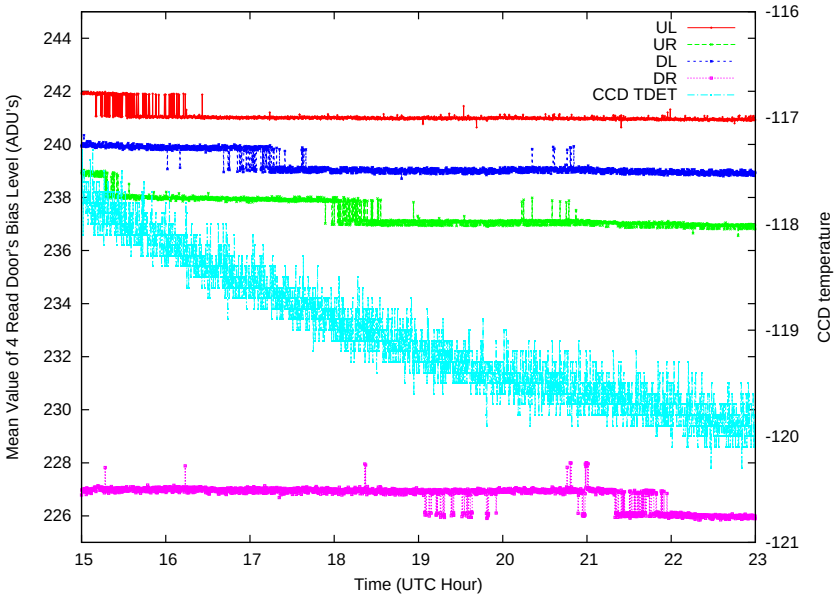

Fig. 6 Four amplifiers bias level when CCD temperature dropped from –117°C to –121°C, the blue curve shows the CCD temperature. Bias is stable during the observation.

calculated by Image Reduction and Analysis Facility's (IRAF's, provided by NOAO) task *findgain*, based on Equations (1) and (2) (Howell 2000, Jones 2006). The principle is to compare the signal levels and the amount of variation in the two bias and two flat field images.

The chip has four amplifiers, so for each reading speed and gain selection, we tested the gain exact value of each amplifier. The testing was carried out on night of 2017 June 26. For the three reading modes of Fast, Medium and Slow, we have selected different gain options to obtain the actual gain value and readout noise. The results are listed in Table 3. It shows that all the readout noise values are similar to the CCD chip nominal value, as given in Table 2.

$$\mathrm{Gain} = \frac{(\overline{F1} + \overline{F2}) - (\overline{B1} + \overline{B2})}{\sigma^2_{F1-F2} - \sigma^2_{B1-B2}} \quad (1)$$

$$\mathrm{Readoutnoise} = \frac{\mathrm{Gain} \cdot \sigma_{\overline{B1}-\overline{B2}}}{\sqrt{2}} \quad (2)$$

3.3 Dark current

On the nights of 2018 June and July, we took the dark current data for the whole night. The measured dark currents of four amplifiers are listed in Table 4, the fitting images are listed in Figure 7. From the test data, dark current signal is so small that we cannot get the dark generate rate when the integral time less than 1800 s. We use the high gain to detect the dark current value, the CCD temperature varied between –100°C and –104°C during the test. The dark data were taken with the exposure time 3600 s and 7200 s. For each exposure time, three frames were taken and more bias was used for correction. Hence, we got the mean and standard deviations from each image. One can see that the dark currents approach the product's manual.

3.4 Linearity

For high precision photometry, the CCD's linearity is very important. To accurately test the response's linearity of camera, measurements were carried out over two nights in June 2017 with dome flats. We took the measurements at night because the stray light will change with the Sun's movement in the daytime. When dusk came, we first closed the cupola. Then, we used A4 paper to adjust the brightness of the incandescent lamp in the dome, made the light homogeneous and dim enough for the CCD camera that could be take long time exposure. One test is the linearity of the full well, the other test is the linearity of the A/D conversion. The mean ADU values were counted based on a 400× 400 region close to CCD center of each amplifier area.

For the full well test, we set CCD linearity with medium read out speed and gain of 3.6. The exposure was set from 0 s to 90 s. The mean count increased with the exposure time, after CCD pixels reached full well, the mean ADU value deviate the main fit line. In Figure 8, we can get that the linearity peak is larger than 36 000, the peak value multiplied by 3.63 equals 130 635 ($>$ 130 000). So, the full well linearity of the CCD camera is better than 99.999%.

Table 3 Test Results About Gain and Readout Noise

Models	Amplifiers	Gain(e^- ADU^{-1})	Readout Noise(e^-)
Fast (146Kpix s^{-1} G 0)	UL	0.980	3.030
	UR	0.970	3.515
	DL	0.990	4.345
	DR	0.980	4.150
Fast (146Kpix s^{-1} G 1)	UL	0.470	2.790
	UR	0.460	3.440
	DL	0.470	4.425
	DR	0.460	4.220
Fast (146Kpix s^{-1} G 2)	UL	0.210	2.740
	UR	0.200	3.340
	DL	0.210	4.290
	DR	0.210	4.010
Medium (91Kpix s^{-1} G 0)	UL	3.610	4.380
	UR	3.585	4.430
	DL	3.680	4.755
	DR	3.640	4.840
Medium (91Kpix s^{-1} G 1)	UL	1.675	2.885
	UR	1.660	3.110
	DL	1.715	3.375
	DR	1.695	3.400
Medium (91Kpix s^{-1} G 2)	UL	0.755	2.525
	UR	0.755	2.640
	DL	0.775	3.005
	DR	0.770	3.010
Slow (51Kpix s^{-1} G 0)	UL	1.590	2.610
	UR	1.455	2.435
	DL	1.620	2.770
	DR	1.500	2.740
Slow (51Kpix s^{-1} G 1)	UL	0.830	2.360
	UR	0.800	2.335
	DL	0.835	2.530
	DR	0.810	2.660
Slow (51Kpix s^{-1} G 2)	UL	0.390	2.270
	UR	0.390	2.300
	DL	0.400	2.430
	DR	0.390	2.680

Table 4 The Dark current of four amplifiers for Slow Reading speed and Gain 2

Amplifier	Dark current (ADU $pixel^{-1}$ s^{-1})	Dark current (e^- $pixel^{-1}$ $hour^{-1}$)
UL	0.000092 ± 0.0000276	0.1325 ± 0.03974
UR	0.000135 ± 0.0000331	0.1944 ± 0.04766
DL	0.000135 ± 0.0000344	0.1944 ± 0.04954
DR	0.000163 ± 0.0000360	0.2347 ± 0.05198

Table 5 Landolt Standards Used in 2017

Star-Name	α (2000)	σ (2000)	V	$B-V$	$U-B$	$V-R$	$R-I$	$V-I$
GD 310C	11:29:25	+38:06:12	13.911	+0.892	+0.668	+0.496	+0.426	+0.924
GD 310A	11:29:29	+38:09:14	14.057	+0.540	–0.073	+0.341	+0.356	+0.698
GD 310B	11:29:35	+38:08:12	14.200	+0.978	+0.832	+0.595	+0.541	+1.137
SA 32–166	12:56:08	+44:00:55	16.316	+0.522	–0.165	+0.409	+0.337	+0.895
…	…	…	…	…	…	…	…	…

For linearity of the A/D conversion, we set CCD parameters with reading speed of Medium and Gain 1, which the gain values approached 1.69 according to Table 3. The exposure time was set from 0 s to 50 s. After the AD converter saturated at 65 535, the 16 bit ADU value decreases as shown in Figure 9. The electron count is close to 110 000 and is far from the full well of 130 000, but we understand that the A/D conversion reached its limit.

4 CALIBRATION OF PHOTOMETRY

The magnitudes which we obtain directly from the images of the CCD cameras are commonly called instrumental magnitudes. If observers plan to cross the NOWT result with history database or other telescope, then they need to know the calibrate coefficients of the NOWT instrumental magnitudes to standard system. In May and August 2017, we selected dozens of standard stars from Landolt catalog

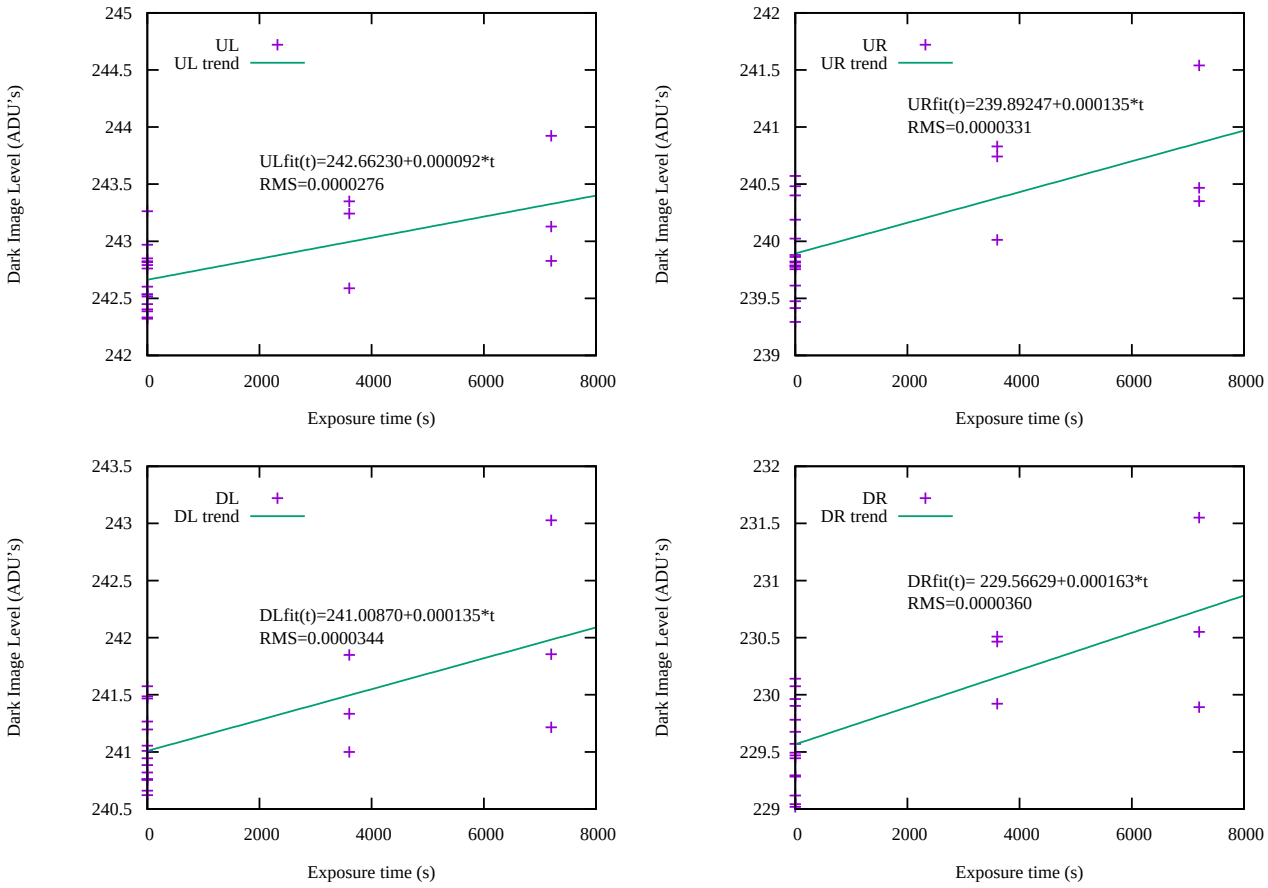

Fig. 7 Dark current of four amplifiers for Slow Reading speed and Gain 2.

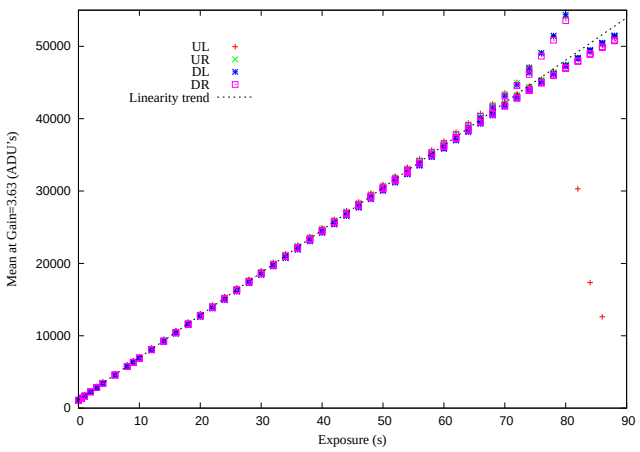

Fig. 8 Mean vs exposure with CCD reading speed of Medium with Gain 0.

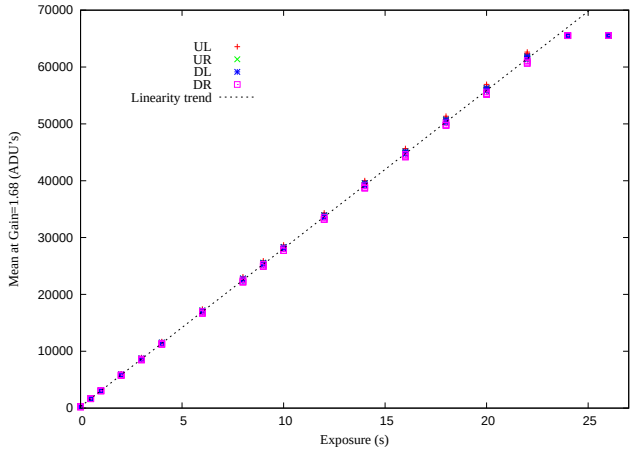

Fig. 9 Mean vs exposure with CCD reading speed of Medium with Gain 1.

(Landolt 1992, Landolt 2013) which are listed in Table 5, considering both the magnitude and colors. Only some of the standards are listed in Table 5. For all the targets has been observed, please refer to the appendix. Some of standard stars can pass the Nanshan Station's zenith, so they are very suitable for calibration.

On observation night, the seeing values approximated 2.0″. After collecting all of the standard stars photometric data, we used the standard photometry steps in *apphot* package to reduce all images in IRAF, which the aperture was set two times of seeing, while 25 is taken as zero point of instrumental magnitudes. Then we obtained the airmass,

instrumental magnitudes and errors. The transformation equations was defined as follows,

$$U_i = U_s + Z_U + K_U^{'}X + C_U(U-B)_s \quad (3)$$
$$B_i = B_s + Z_B + K_B^{'}X + C_B(B-V)_s \quad (4)$$
$$V_i = V_s + Z_V + K_V^{'}X + C_V(B-V)_s \quad (5)$$
$$R_i = R_s + Z_R + K_R^{'}X + C_R(V-R)_s \quad (6)$$
$$I_i = I_s + Z_I + K_I^{'}X + C_I(V-I)_s \quad (7)$$

where U_s, B_s, V_s, R_s and I_s are the Landolt standard magnitudes, U_i, B_i, V_i, R_i and I_i are the NOWT instrumental magnitudes, Z_U, Z_B, Z_V, Z_R and Z_I are zero point magnitudes of NOWT, $K_U^{'}$, $K_B^{'}$, $K_V^{'}$, $K_R^{'}$ and $K_I^{'}$ are the first-order coefficients of extinction , C_U, C_B, C_V, C_R and C_I are the color terms in the transformation equations, and X denotes the airmass.

On each test night, we got more than 40 frames data for each band. Each frame contains more than five standard stars on average, so for each band we have more than 200 records. Then, we derived the coefficients and fitted the observed magnitudes with *mknobsfile* and *fitparams* tasks in the *photcal* package in IRAF. The second-order terms of extinction were too small, so it has been ignored. We obtained transformation coefficients based on Equations from (3) to (7), including the zero points (Z), filter names, first-order extinction coefficients ($K^{'}$), filter names, root mean square (RMS) values and color terms (C), these parameters are listed in Table 6. We compare our calibration coefficients with results of Xinglong station in Table 7. One can see that some coefficients are smaller, possibly because the altitude of Nanshan Station is higher.

Figure 10 shows a comparison between the transformation equations in $UBVRI$ bands and the Landolt standard magnitudes.

Using the transformation coefficients and the data which were taken in August 2017 and May, the relationship between the Landolt standard and the shifted calibration were derived. From Figure 10, we can see that the slopes of all fitted lines are close to 1.0. As listed in Table 6, the magnitude rms in each filter is smaller than 0.13. It indicates that the calibration between NOWT's photometric system and the Johnson system is established well.

5 OVERALL PERFORMANCE

5.1 Throughput

By observing several Landolt standards, the entire optical system's total throughput can be estimated. Beside atmospheric transformation, quantum efficiency of camera and and filter response, the throughput also includes correctors and primary mirror reflection. The throughput of Lulin Observatory was tested by the method (Kinoshita et al. 2005) that has been introduced by Kinoshita. The NOWT's throughput efficiency is calculated based on the flux of Vega (Bohlin & Gilliland 2004, Bohlin 2014) that followed Equation (8), which was introduced by Fan (Fan et al. 2016).

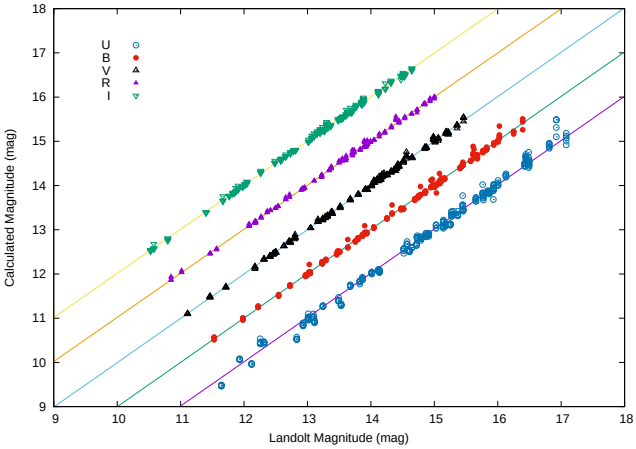

Fig. 10 Transformed magnitudes versus Landolt standards using derived transformation coefficients in five bands. The U, B, R, I bands transformed magnitudes are shifted to –2, –1, +1, +2 magnitudes. The best linear fits were represented with solid lines.

$$\eta(\lambda) = \frac{F_{\rm ADU} \cdot G}{F_\lambda \cdot \delta\lambda \cdot S_{\rm tel}}, \quad (8)$$

where $F_{\rm ADU}$ is the counts of standard star per second (ADU s^{-1}); from the standard star's AB mag, we can derive its theoretical photon number F_λ of per second (photon s^{-1} cm^{-2} $Å^{-1}$); G represents the gain of camera (e^- ADU^{-1}); $\delta\lambda$ is the grating dispersion of spectroscopic observations or the effective band of the filter in photometric observations (Å); λ is the wavelength used to compute the efficiency of spectroscopy or the effective wavelength for filters (Å) and $S_{\rm tel}$ is the primary mirror's effective area (cm^2).

Table 8 lists the median throughput of five bands. Because our CCD chip is a blue sensitivity kind, the efficiency of blue side is higher than the red side. We cleaned the main mirror before entering the winter, so the efficiency of March 2018 is higher than May 2017.

5.2 Photometry Accuracy And Limits

The sky brightness at Nanshan Station has been introduced by Hu (Hu et al. 2017). Equation (9) is enable us to make the estimation (Howell 2000).

Table 6 Coefficients and Standard Deviation of NOWT Photometric System

Date	Filter	Zero points (Z)	Extinction ($K^{'}$)	Color Term (C)	RMS
2017–5–03	U_i	4.801 ± 0.039	0.496 ± 0.032	–0.166 ± 0.010	0.132
2017–5–04	U_i	4.844 ± 0.036	0.540 ± 0.029	–0.167 ± 0.009	0.126
2017–8–29	U_i	4.782 ± 0.015	0.550 ± 0.011	–0.045 ± 0.009	0.072
2017–5–03	B_i	1.987 ± 0.015	0.256 ± 0.012	–0.024 ± 0.006	0.061
2017–5–04	B_i	2.060 ± 0.019	0.264 ± 0.015	–0.030 ± 0.006	0.062
2017–8–29	B_i	1.958 ± 0.007	0.359 ± 0.005	–0.014 ± 0.003	0.042
2017–5–03	V_i	2.181 ± 0.013	0.166 ± 0.010	0.013 ± 0.005	0.047
2017–5–04	V_i	2.184 ± 0.012	0.216 ± 0.010	0.014 ± 0.004	0.040
2017–8–29	V_i	2.154 ± 0.006	0.258 ± 0.004	0.012 ± 0.002	0.029
2017–5–03	R_i	2.317 ± 0.015	0.104 ± 0.012	0.019 ± 0.009	0.053
2017–5–04	R_i	2.312 ± 0.015	0.156 ± 0.012	0.019 ± 0.008	0.050
2017–8–29	R_i	2.281 ± 0.007	0.192 ± 0.005	0.027 ± 0.005	0.034
2017–5—03	I_i	3.274 ± 0.012	0.078 ± 0.010	0.012 ± 0.004	0.047
2017–5–04	I_i	3.255 ± 0.013	0.128 ± 0.010	0.013 ± 0.004	0.044
2017–8–29	I_i	3.246 ± 0.005	0.143 ± 0.003	0.011 ± 0.002	0.023

Table 7 Extinction Coefficients at Nanshan Station

Year	$K^{'}_U$	$K^{'}_B$	$K^{'}_V$	$K^{'}_R$	$K^{'}_I$	Ref
2016	0.590±0.022	0.431±0.029	0.282±0.026	0.217±0.019	0.156±0.021	(Bai et al. 2018)
2011–2012		0.348±0.022	0.236±0.017	0.168±0.019	0.085±0.021	(Huang et al. 2012)
2008		0.330±0.007	0.242±0.005	0.195±0.004	0.066±0.003	(Zhou et al. 2009)
2006–2007		0.307±0.009	0.214±0.008	0.161±0.008	0.091±0.008	(Huang et al. 2012)
2004–2005		0.296±0.012	0.199±0.009	0.141±0.010	0.083±0.009	(Huang et al. 2012)

Table 8 The Total Throughput of NOWT in $UBVRI$ Bands

Date	U	B	V	R	I
2017–05–03	5.4%	25.8%	31.4%	25.4%	15.6%
2018–03–10	6.1%	30.9%	38.6%	30.6%	18.2%

$$\mathrm{SNR} = \frac{N_{\mathrm{star}}}{\sqrt{N_{\mathrm{star}} + n_{\mathrm{pix}}(N_{\mathrm{sky}} + N_{\mathrm{dark}} + N^2_{\mathrm{readout}})}} \quad (9)$$

$$\sigma = 1.0857/\mathrm{SNR}\,, \quad (10)$$

where N_{star} is the total photons of target, n_{pix} is the pixels number under certain seeing condition, N_{sky} is the sky background total number on each pixel, N_{dark} is the dark current per pixel land, N_{readout} is the readout noise listed in Section 3.2. The dark current's effect is extremely small, so it is neglected here. The photometric error can get easily from SNR, as σ in Equation (10). The correction term between error and electron in magnitude is 1.0857.

To check the calibration relationship's reliability, observations were carried out by targeting globular cluster M13 during several nights in May 2017. To obtain the relationship between the exposure time, magnitude and signal-to-noise ratio, this part of the work is based on the IRAF standard photometric results. First, we took short exposure for each band, and then aligned and combined the image after preprocessing. The purpose is to improve the signal-to-noise ratio and avoid pixel saturation. The corresponding exposure time for each band was 600 s for U, 12 s for B, 144 s for V, and 72 s for R and I bands. In Figure 11, the relationship between the photometry error of long time exposure and transformed stars brightness of different bands is shown. The photometry error of the I band corresponding to the magnitude is lower than other bands, and even lower than the U band. The main reason is that our CCD camera is blue sensitive.

We then set the exposure time of M13 with V band to 72 s, and took two images in a row. Then, photometry information of all stars was acquired, which SNR must be higher than 2. In Figure 12, the photometric accuracy (errors $\triangle V$) versus magnitude of the two independent measurements is plotted. The result is similar to the one meter telescope at Weihai Observatory (Hu et al. 2014) and Xinglong Station (Bai et al. 2018).

Different exposure times were made for each filter with five sets in the whole photometric night (clear, breeze and no Moon). During the observation loops, the airmass of each star field was changing. After we got the image and standard reduction, photometric accuracy and magnitude was obtained with different airmasses for each band. So, we can derive the relationship between the SNR of the limiting magnitudes changing with the airmass and exposure time. In Figures 13 and 14, the limiting magnitude versus the exposure time is plotted with SNR of 100 and 200. Observers can estimate their targets'

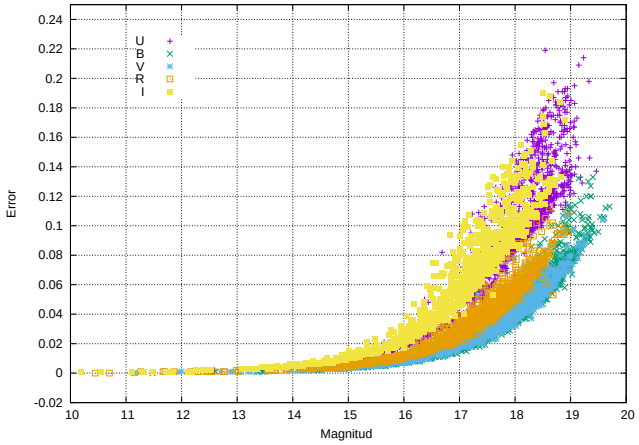

Fig. 11 Photometry error versus transformed magnitude of M13 with 600 s for U, 120 s for B, 144 s for V, 72 s for R and I bands, respectively.

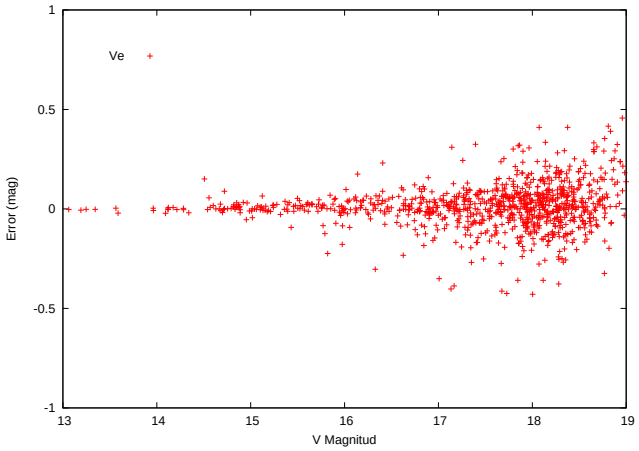

Fig. 12 Photometric accuracy errors of the two independent measurements in the V band. The exposure time is 72 s.

exposure time by using these figures. Based on previous observations, we simulated the 300-second exposure when the telescope was aimed at the zenith. The simulated results with SNR of 5 are 19.0, 21.2, 21.3, 20.9 and 20.5 mag in the U, B, V, R and I bands, respectively.

6 SUMMARY

NOWT's photometric system is introduced in this paper. To offer more valuable information for users, the readout noise, bias, dark current, gain and linearity of the CCD camera are tested. One can get that the camera has a very good scientific-grade CCD from the test results. We selected dozens of Landolt standards for multiple night observations in different seasons. Based on the test data, the transformation coefficients are derived between the standard magnitude and the instrumental $UBVRI$

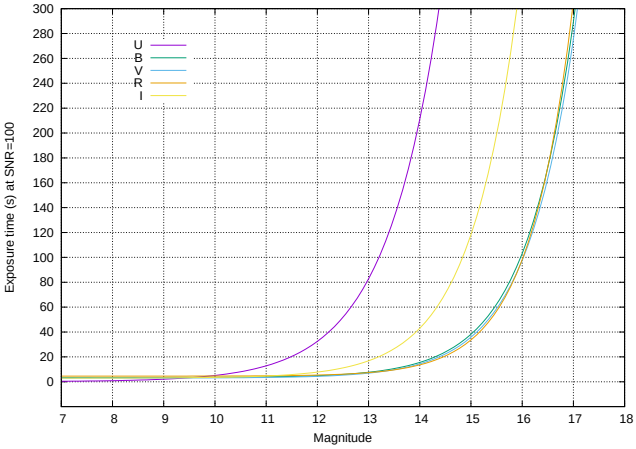

Fig. 13 Exposure time requirement of limiting magnitude when SNR is 100.

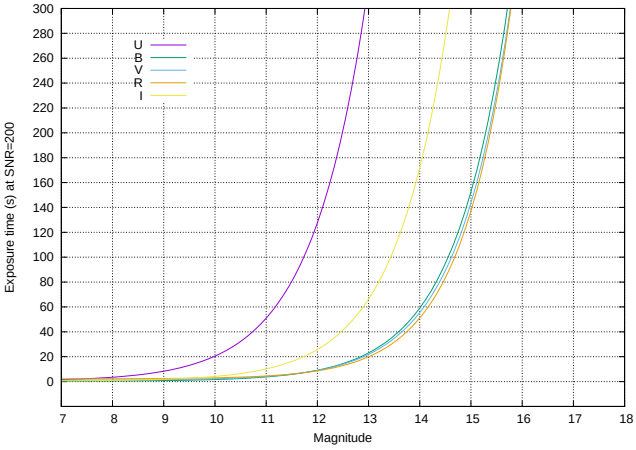

Fig. 14 Exposure time requirement of limiting magnitude when SNR is 200.

magnitude. The color terms and atmospheric extinction coefficients are found and compared with the results of the other stations. Due to the blue sensitivity chip and the altitude of Nanshan Station, the NOWT's throughput is good, especially on the blue side. The limiting magnitude can reach 19.0, 21.2, 21.3, 20.9, 20.5 mag in corresponding five bands with the exposure of 300 s and SNR of 5. Finally, we give guidance regarding exposure to observers about the limiting magnitude at different exposure time and SNR requirement.

Acknowledgements We gratefully acknowledge the support of the staff of the NOWT. This research is supported by the program of the light in China's Western Region (LCWR; Grant Nos. 2015-XBQN-B-04, 2015-XBQN-A-02), the National Natural Science Foundation of China (Grant Nos. 11803076, 11873081, 11661161016 and U1831209), the 13th Five-year Informatization Plan of Chinese Academy of Sciences (Grant No. XXH13503–03–107), the Youth Innovation Promotion Association

CAS (Grant Nos. 2014050, 2018080), and the Strategic Priority Research Program of the Chinese Academy of Sciences (Grant No. XDB23040100), 2017 Heaven Lake Hundred-Talent Program of Xinjiang Uygur Autonomous Region of China and the Open Project Program of the Key Laboratory of Optical Astronomy (NAOC).

References

Bai, C.-H., Fu, J.-N., Li, T.-R., et al. 2018, RAA (Research in Astronomy and Astrophysics), 18, 107
Bai, C.-H., Ji-Lin, Z., Feng, G.-J., et al. 2019, Astronomical Research and Technology, 16, 488
Bohlin, R. C. 2014, AJ, 147, 127
Bohlin, R. C., & Gilliland, R. L. 2004, AJ, 127, 3508
Fan, Z., Wang, H., Jiang, X., et al. 2016, PASP, 128, 115005
Fu, J. N., Vauclair, G., Su, J., et al. 2017, in Astronomical Society of the Pacific Conference Series, Vol. 509, 20th European White Dwarf Workshop, ed. P. E. Tremblay, B. Gaensicke, & T. Marsh, 355
Howell, S. B. 2000, Handbook of CCD Astronomy (2nd Ed. Cambridge: Cambridge Univ. Press, 2006)
Hu, P., Li, R., Wang, N., & Wei, P. 2017, Astronomical Research and Technology, 14, 495
Hu, S.-M., Han, S.-H., Guo, D.-F., & Du, J.-J. 2014, RAA (Research in Astronomy and Astrophysics), 14, 719
Huang, F., Li, J.-Z., Wang, X.-F., et al. 2012, RAA (Research in Astronomy and Astrophysics), 12, 1585
Jones, D. 2006, The Observatory, 126, 379
Kinoshita, D., Chen, C.-W., Lin, H.-C., et al. 2005, ChJAA (Chin. J. Astron. Astrophys.), 5, 315
Landolt, A. U. 1992, AJ, 104, 340
Landolt, A. U. 2013, AJ, 146, 131
Liu, J., & Zhang, Y. 2016, in IAU Symposium, 312, Star Clusters and Black Holes in Galaxies Across Cosmic Time, eds. Y. Meiron, S. Li, F. K. Liu, & R. Spurzem, 296
Liu, J., Zhang, Y., Feng, G., & Bai, C. 2014, in IAU Symposium, 298, Setting the Scene for Gaia and LAMOST, eds. S. Feltzing, G. Zhao, N. A. Walton, & P. Whitelock, 427
Ma, S.-G., Esamdin, A., Ma, L., et al. 2018, Ap&SS, 363, 68
Wang, S., Wu, D.-H., Addison, B. C., et al. 2018, AJ, 155, 73
Yang, T.-Z., Esamdin, A., Fu, J.-N., et al. 2018, RAA (Research in Astronomy and Astrophysics), 18, 002
Zhang, X.-F., Liu, J.-Z., Jeffery, C. S., Hall, P. D., & Bi, S.-L. 2018, RAA (Research in Astronomy and Astrophysics), 18, 009
Zhang, Y., Liu, J., & Zhang, F. 2015, MNRAS, 449, 3301
Zheng, J., Zhao, G., Wang, W., et al. 2019, RAA (Research in Astronomy and Astrophysics), 19, 003
Zhou, A.-Y., Jiang, X.-J., Zhang, Y.-P., & Wei, J.-Y. 2009, RAA (Research in Astronomy and Astrophysics), 9, 349